An Ensemble Learning-Based Prediction Model for Image Forensics From IoT Camera in Smart Cities

GE XU[1,3], YONGQIANG XIAO[2], TAO WANG[1,3,4], (Member, IEEE), YIN GUAN[1], JINHUA XIAO[2], ZHIXIONG ZHONG[1], (Member, IEEE), DONGYI YE[3], AND JIA LYU[5]

[1]Fujian Provincial Key Laboratory of Information Processing and Intelligent Control, College of Computer and Control Engineering, Minjiang University, Fuzhou 350108, China
[2]Fuzhou Kaopuyun Technology Company Ltd., Fuzhou 350001, China
[3]College of Mathematics and Computer Science, Fuzhou University, Fuzhou 350108, China
[4]Key Laboratory of Cognitive Computing and Intelligent Information Processing of Fujian Education Institutions, Wuyi University, Wuyishan 354300, China
[5]College of Clothing and Artistic Engineering, Minjiang University, Fuzhou 350108, China

Corresponding author: Tao Wang (taowang2600@gmail.com)

ABSTRACT Recent years witnessed a surge in the number of IoT cameras in smart cities. In this article, an ensemble learning-based prediction model for image forensics from IoT camera is proposed. In particular, our goal is to obtain human body measurements from 2D images taken from two views. Firstly, 24 body part features are extracted by the DensePose algorithm from the two views. Secondly, the features of the upper body part are integrated with height and body weight features. Ensemble learning is then performed with the LightGBM algorithm and a regression prediction model is constructed. The proposed noncontact image prediction method is simple and workable. Its feasibility and validity are verified on an experimental dataset. Experimental results demonstrate that the proposed method is highly reliable in the size prediction of different body parts. Specifically, the mean absolute errors of chest circumference, waistline and hip circumference are about 2.5 cm, while the mean absolute errors of other predictions are about 1 cm.

INDEX TERMS Human body part measurements, ensemble learning, regression prediction.

I. INTRODUCTION

In recent years, IoT cameras have become ubiquitous in smart cities, and these sensors are widely adopted for forensic applications [1], [2]. One of the important application areas is the measurements of the human body for places where strong security is needed. In particular, the ability to acquire human body measurements, i.e., anthropometry, in a noncontact manner is highly desired. In this article, we propose an ensemble learning-based prediction model that allows forensic evidence to be extracted from images both efficiently and effectively. Noncontact human body size measurement of different body parts based on the static images which are taken by cameras not only can improve

user experiences, but also can save material and financial costs. With the informatization development in the clothing industry, intelligent anthropometry will lay a solid foundation for the next generation of intelligent dressing recommendation [3]. Nowadays, offline flow still owns a great space with the development of AIoT [4]–[6]. For example, users can try more clothes in a short period through the emerging virtual fit [7]. As one of the key technologies in virtual fit, anthropometry acquires measurement data of main body parts accurately in a relatively simple way. Virtual fit products on the market include Fitiquette (USA), Fits.me (UK) and Pulshion (China). All of these products generally require users to fill in relevant body sizes firstly, then generate the corresponding 3D anthropometric dummy, and finally render the dressing effect onto the 3D anthropometric dummy [8]–[10]. For these products, precision of body size data which is input by users

The associate editor coordinating the review of this manuscript and approving it for publication was Kun Wang.

can affect the reliability of online fitting directly. Nevertheless, users often are not sure about their accurate body sizes. Obviously, contact manual measurement of body sizes will affect user experiences. Therefore, the precision of noncontact anthropometry is vital to the practicability of clothing-related applications [11].

Although many high-precision anthropometric 3D scanners based on depth transducers like structural lights have been applied successfully in intelligent noncontact anthropometry, the device still faces with a great challenge to large-scale applications in the clothing industry, especially in small-sized clothing enterprises, due to its low popularizing rate [12]. Hence, it is urgent to propose an economic and convenient intelligent noncontact anthropometry. To meet the above demands, a simple and feasible intelligent anthropometry method was proposed in this study. The proposed method establishes a regression model based on DensePose [13] algorithm by combining real body detection results in images, image features of the human body and features of height and body weight. It can predict different body sizes accurately from end to end under casual shooting requirements and decrease accumulative errors brought by intermediate links, such as extraction of key points.

II. RELATED WORK

Artificial intelligence plays an important role in smart cities [14], [15]. Particularly, studies on noncontact anthropometry have begun in foreign countries since the late 1970s [16]. In the beginning, noncontact anthropometry was performed in USA and UK by using some large computing devices, which incurs relatively high costs [7]. One of the main benefits for anthropometry is that it would facilitate biomechanical analysis and human motion (e.g., [17]–[19]). In particular, the emerging IoT cameras allow for large-scale imagery data to be collected with low cost and used as forensic evidence when needed. Typically and conventionally, computer vision-based anthropometry use 3D scanners [20]–[26]. This is, however, in contrast to our goal in this article. We propose to collect image data with low-cost IoT cameras and therefore an algorithm that can make use of 2D images only and then produce reliable human body measurements is desired.

Without using large-sized 3D human body scanners, two-dimensional images of human body were collected firstly based on digital image processing and then processed generally through corrosion, expansion, smoothing, edge sharpening, etc. These operations are to extract the accurate profiles of human body for the convenience of next point extraction, measurement and computation. There's a difficulty in measurement and computation: how to calculate the nonlinear circumferences of human body. At present, calculation methods of circumferences mainly include curve fitting, regression analysis [27]–[30] and minimizing appropriate cost functions [31]–[33]. One of the limitation of purely 2D-based methods is that, it could only estimate a human's anthropometric measurements up to a scale parameter. In our work,

we circumvent this problem by asking the user to provide their body height and weight as prior information.

Tan [34] and Ji *et al.* [35] extracted characteristic points of body parts by taking pictures of human body and then calculated circumferences through curve fitting. This method had certain research values. Yu *et al.* [36] also took pictures and then processed them accordingly. They mainly acquire the profiles of human body through greyscale inversion. Circumference values also could be calculated by demonstrating the calculation formula, which further solves the difficulties in circumference calculation.

Recently, many studies adopt fitting binary regression equation to calculate circumferences [12], [37], [38]. This method firstly sets up the linear relationship between the width and thickness of body parts and circumferences. Secondly, it divides the human body into different levels according to the thickness-width ratio to be corresponding to parameters of the linear equation. Finally, it makes a statistics on fitting linear equation based on mass data. Although this method is simple, the generalized anthropometric precision is generally low. Another modeling theory is to cite the double elliptic curve fitting or hyperelliptic curve fitting [39]. Although this method is well supported by a good fundamental theory and offers a relatively controllable precision, it requires mass statistical data since it is difficult to determine the model coefficients. Hence, this method is impractical.

Currently, researches on anthropometry have to search the corresponding characteristic points. However, it always cannot search characteristic points accurately, especially in casual shooting scenes where dressing can influence measurement precision. The main contribution of this study, therefore, is to propose a deep learning based method for anthropometry. Considering common features of human body and understandability of human body, deep learning can extract information of different body parts effectively and it can establish an end-to-end regression model to predict body sizes by combining the integrity of human body. Compared with the conventional method, the proposed anthropometry method is simpler and more feasible and has lower requirements on shooting. It only requires the positive and side views. Therefore, the proposed anthropometry method is highly practical.

III. THE PROPOSED METHOD
A. INTELLIGENT NONCONTACT ANTHROPOMETRY

A flowchart of the proposed noncontact anthropometry based on two views is shown in Fig.1. One front picture and one side picture of the human body are taken firstly by using the ordinary color camera lens. Secondly, 24 features of body parts were extracted by the trunk network division model which is pretrained by Dense Pose algorithm. Meanwhile, features of height and body weight are integrated as the feature input of the ensemble learning framework LightGBM. The Boosting algorithm of LightGBM predicts the circumferences of human body by using the GBDT [40] learning regression, and learns the importance of statistical features automatically in
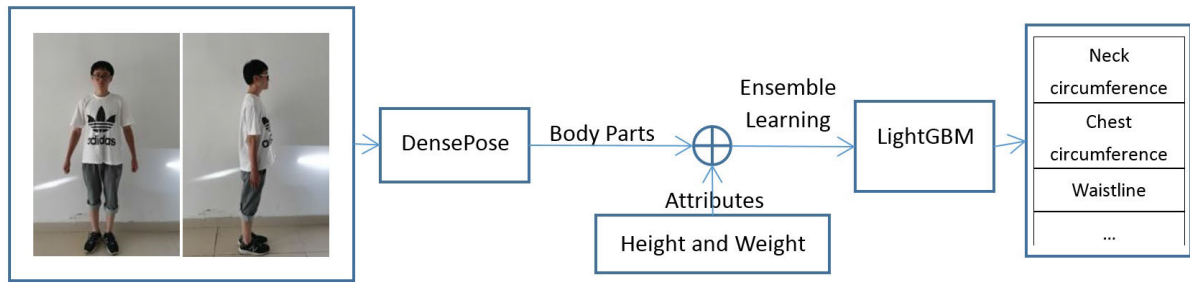
FIGURE 1. The proposed prediction model for intelligent noncontact anthropometry for image forensics. Images from frontal and side views are provided as input to the DensePose algorithm. The output features, together with body height and weight, are fed into LightGBM for ensemble learning based prediction.
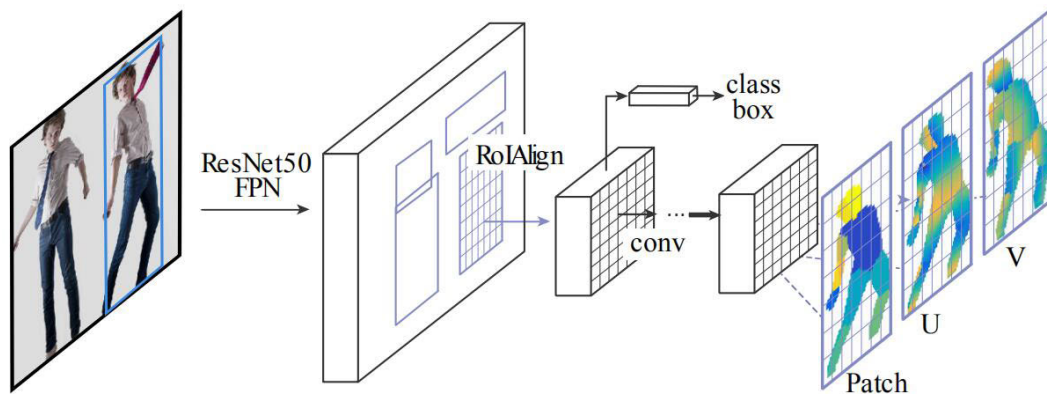

FIGURE 2. Model structure in DensePose-RCNN. Features are extracted from region CNNs to produce body parts (Patch) and texture (UV) maps.

the training stage. It has characteristics of high speed, small hardware resource consumption, light model in the prediction stage, and easy migration, deployment and recalling.

The proposed method requires neither extraction of profile information of human body through various fundamental image processing operations nor extraction of key points of body parts to calculate circumference values. These have advantages of reducing artificial engineering design during the algorithm process as well as the accumulation of possible errors. The proposed anthropometry method can be promoted to various practical applications due to its simplicity.

B. HUMAN BODY INFORMATION EXTRACTION BASED ON DensePose

DensePose algorithm is an intensive body posture estimation by Facebook and INRIA together to realize an understanding of human body in images. Generally speaking, this framework can understand the human body in casual dressing accurately and accurate different body parts.

It can be seen from Fig.2 that DensePose makes intensive prediction of body parts (Patch) and UV texture maps after body examination by using the full convolutional network [41]. Heat mapping features of Patch, U and V are 56×56. The value range of Patch is $[0,24]$, while the value range of U and V is $[0,1]$. It can be seen from Fig.3 that the

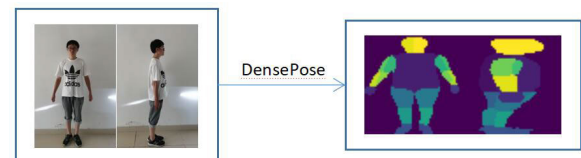**FIGURE 3.** 56×56 heat map features of Patch channel.

number of features which are extracted by DensePose from the positive and side views of Patch is $(56 \times 56 + 6) \times 2 = 628$, where 6 represents the positional information of human body in the original image as well as width and height of the frame.

In this experiment, it compares the effects of using features of Patch channel only and the effects of adding features of UV channels. It is found that the predicted values of each circumference indexes were basically the same no matter whether the features of UV channels were added in or not. Therefore, this study used the features of Patch channel only to prevent increasing hardware resource consumption because of the excessive dimensions of features. Moreover, DensePose was proved to be poor in predicting the data of head, palms and soles of human body. Hence the influences of these three body parts on the prediction precision of circumferences were compared. Results demonstrated that these three body parts hardly influenced the prediction precision of circumference indexes.
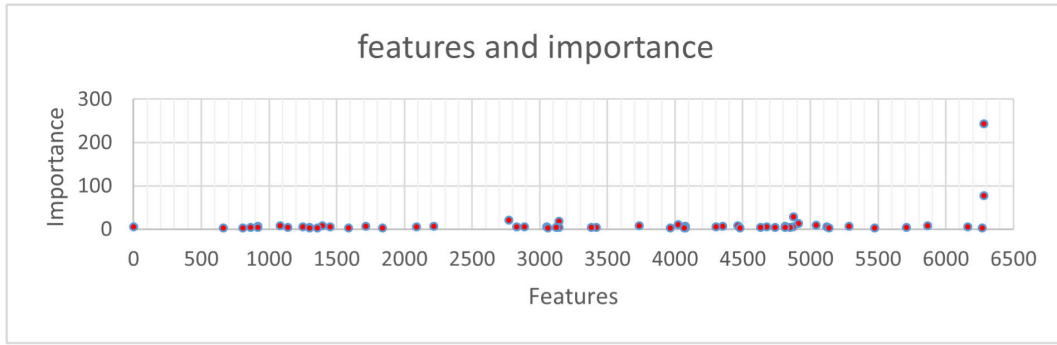
FIGURE 4. Top 60 points after sequencing of features and importance.

C. ESTABLISHING A REGRESSION PREDICTION MODEL BY INTEGRATING IMAGE AND ATTRIBUTE FEATURES

LightGBM was launched by Microsoft in 2017. As an improved version of XGBoost [42], LightGBM decreases the time complexity of sample processing and improves the expandability of the algorithm. In this study, the LightGBM algorithm was applied mainly for effectively selecting the high-dimensional features extracted by DensePose algorithm, thus resulting in reducing the feature complexity and assuring precision of body size prediction.

Through a comparative experiment, this study combined eigenvectors of images, height and body weight as the feature input of LightGBM. Besides, GBDT used boosting and the target loss function applied the root-mean-square error (RMSE) and mean absolute error (MAE):

$$RMSE = \sqrt{\frac{1}{N}\sum_{i=1}^{N}(p_i - y_i)} \qquad (1)$$

$$MAE = \sqrt{\frac{1}{N}\sum_{i=1}^{N}|p_i - y_i|} \qquad (2)$$

where p_i refers to the predicted value, y_i refers to real manually measured value and N is the number of samples.

The top 60 points obtained in the hipline prediction model of adult males are shown in Fig.4. In the experimental results, the importance of 6286 input features was examined and the body weight was proved to be the most important index (often occupied the top position) during the construction of each body part prediction model. Differently, the height takes the front ranks according to the importance, but its rank was unstable. For example, the 6285th and 6284th features in Fig.4 represent height and body features. Attentions shall be paid to that the subscripts of features were counted from 0.

IV. EXPERIMENTS
A. EXPERIMENTAL PLATFORM AND DATASET
The experimental platform includes the mobile end and service end. The mobile end in Fig.5 mainly shoots front and back images of human body. It is equipped with an Android or iOS system. Image resolution was unified to
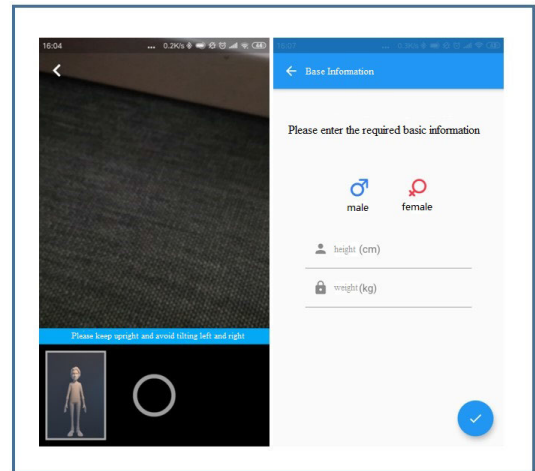

FIGURE 5. The image collection mobile app used in this work.

1080 × 1920. Moreover, input information covers gender, height and body weight. The backstage service end is used for data training and prediction. It is equipped with a Ubuntu 64-bit system, GeForce RTX 2070 8G display card and 24G memory.

In casual scenes, respondents shall be covered completely in lens and no unrelated person is allowed in the background. Respondents are not required to wear tights and they are only required to expose hands, foots and some body weights, without jewelries like watch as much as possible. Front standing posture has a basic requirement of making fists to be slightly away from the body, making two feet slightly away from each other, and eyes looking front. The side standing posture requires respondents to making fists and close to the middle of hips, feet together and eyes looking front.

Collected data were divided into adult males and adult females aged between 20 45. In the measurement, 46 adult males and 59 adult females were invited. Measurement indexes included height, body weight, neck circumference, shoulder width, chest circumference, waistline, hipline, arm circumference, elbow circumference, forearm circumference, wrist circumference, thigh circumference, knee width,

TABLE 1. Indexes and Statistical Data of Adult Males (unit: cm, Body weight: 500g).

| Statistical indexes	Height	Body weight	Neck circumference	Shoulder width	Chest circumference	Waistline	Hipline
Min	156	90	40	40	75	60	79
Max	190	212	49	48	118	111.5	116
Mean	174.1	133.7	43.4	43.9	90	80	95.5
SD	6.8	26.5	2.2	2.2	9.7	10.9	7.9a
Arm circumference	**Elbow circumference**	**Forearm circumference**	**Wrist circumference**	**Thigh circumference**	**Knee width**	**Calf circumference**	**Ankle circumference**
23	22	15.5	15	41	32	31	22
38	29	29	19	61	44	45.5	28.5
28.6	24.7	24.7	16.4	52.5	37.2	36.5	24.4
3.3	1.7	2.4	0.9	4.7	2.7	3.3	1.3
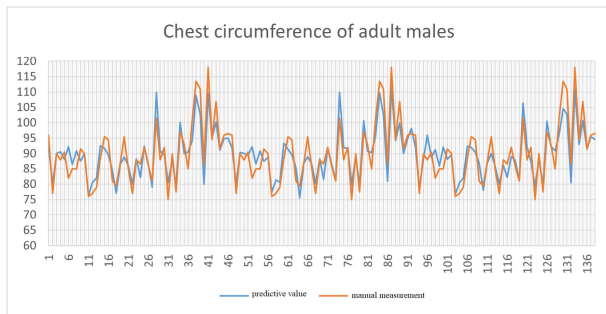
FIGURE 6. Comparison between predicted results and manual measurements of chest circumference of adult males.

FIGURE 7. Comparison between predicted results and manual measurement of waistline of adult males.
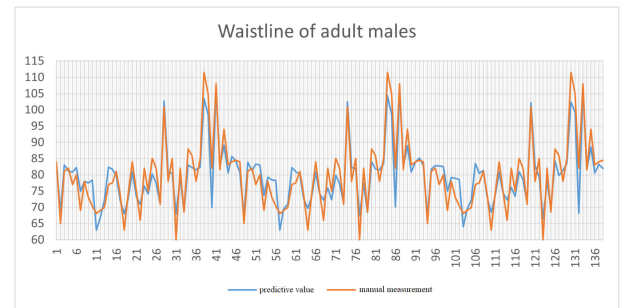

FIGURE 8. Comparison between predicted results and manual measurement of hipline of adult males.

calf circumference and ankle circumference. Among them, the height and body weight were used as input data, while the other 13 indexes were used as the prediction tag values. Manual measurement was adopted and the mean of three measurements was taken. Measuring tools included 2 flexible rules, 2 doctor's type scale, height chart and 3 cell phones. It can be seen from Table 1 and Table 2 that the minimum, maximum, mean and standard deviation of each index measured by 3 cell phones are listed. Body weight used the unit of 500g, and the rest indexes all used the unit of cm. Image data were collected from casual scenes. The total number of male respondents was $46 \times 3 = 138$ and the total number of female respondents was $59 \times 3 = 177$.

B. PREDICTION EXPERIMENTS OF CIRCUMFERENCE INDEXES OF ADULT MALES

The final training strategy was applied: 6-fold validation was performed to data of 46 respondents, and then divided into {8, 8, 8, 8, 7, 7}. Attentions shall be paid that 138 samples were not divided randomly under an unconditional state. Comparisons between the predicted results and manual measurements of chest circumference, waistline and hipline of adult males are shown in Fig.6-Fig.8. The x-coordinate represents the specific sample and the y-coordinate expresses the circumference value. RMSE, MAE, maximum error, minimum error and mean error rate of predicted results and manual measurements of 13 indexes are shown in Table 3.

C. PREDICTION EXPERIMENTS OF CIRCUMFERENCE INDEXES OF ADULT FEMALES

The final training strategy was the same with that of the scenario of adult males: 6-fold cross validation was performed to data of 59 respondents, and then divided into {10,10,10,10,10,9}. Attentions shall be paid that 177 samples were not divided randomly under an unconditional state. Comparisons between the predicted results and manual measurements of chest circumference, waistline and hipline of adult females are shown in Figs.9-11. The x-coordinate represents the specific sample and the y-coordinate expresses the circumference value. RMSE, MAE, maximum error, minimum error and mean error rate of predicted results and manual measurement of 13 indexes are shown in Table 4.
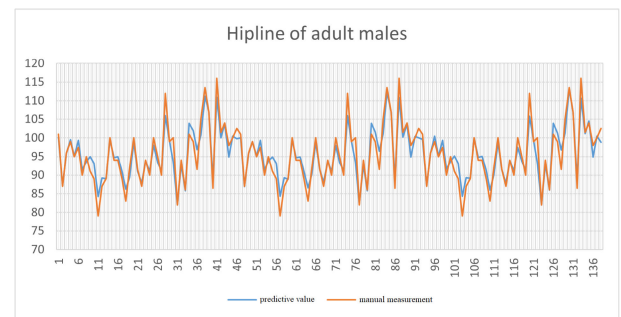
TABLE 2. Indexes and Statistical Data of Adult Males (unit: cm, Body weight: 500g).

Statistical indexes	Height	Body weight	Neck circumference	Shoulder width	Chest circumference	Waistline	Hipline
Min	148	75	32.5	30	74	57.5	80
Max	167	166	42	41	101	86	115
Mean	158.7	107.7	36.2	36.1	85.6	70.3	92.2
SD	4.5	16.8	2	2.2	6.8	6.5	6.2
Arm circumference	**Elbow circumference**	**Forearm circumference**	**Wrist circumference**	**Thigh circumference**	**Knee width**	**Calf circumference**	**Ankle circumference**
21	18.5	19	12.5	44	31	27	17.5
32	26.5	26	18	70	54	44	24
25.2	21.6	21.5	14.4	52.2	35.9	33.8	20.3
2.5	1.5	1.5	1	4.4	3.8	3	1.4

TABLE 3. Indexes and Errors of Adult Males.

| Error indexes	Neck circumference	Shoulder width	Chest circumference	Waistline	Hipline	Arm circumference
RMSE	1.4	1.5	4.2	4.3	2.5	1.9
MAE	1.1	1.2	3.3	3.4	1.8	1.3
Max error	4.8	3.4	10.2	10.8	6.7	7
Min error	0	0	0.02	0.02	0.01	0
Mean error rate	2.50%	2.70%	3.70%	4.20%	1.90%	4.50%
Elbow circumference	**Forearm circumference**	**Wrist circumference**	**Thigh circumference**	**Knee width**	**Calf circumference**	**Ankle circumference**
0.6	1.7	0.5	2.4	1.8	1.6	0.8
0.5	1	0.4	1.9	1.4	1.3	0.6
1.6	8.9	1.4	4.9	4.8	3.4	2.6
0	0	0	0	0	0	0
2.00%	4.00%	2.40%	3.60%	3.70%	3.50%	2.40%
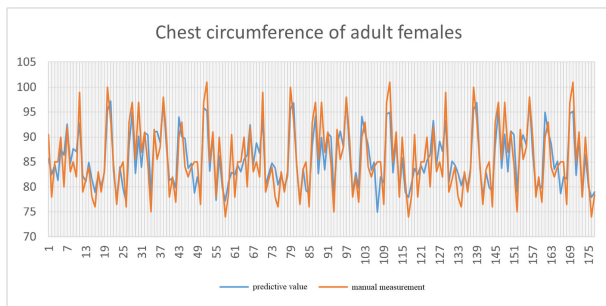
FIGURE 9. Comparison between predicted results and manual measurements of chest circumference of adult females.
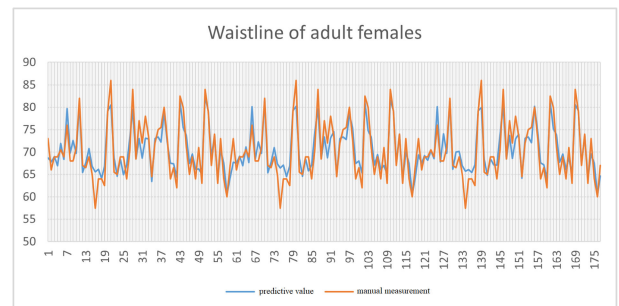

FIGURE 10. Comparison between predicted results and manual measurements of waistline of adult females.

D. RESULTS ANALYSIS

Experimental results about the errors of different indexes of adult males are shown in Table 3. For MAE, the minimum is observed at wrist circumference (0.4cm) and the maximum is achieved by the waistline (3.4cm). Hipline presents the minimum mean error rate (1.9%), while the arm circumference presents the maximum mean error rate (4.5%). The index with high MAE might not have a high mean error rate and vice versa. This is caused by the relatively long length of indexes. Table 1 and Table 3 show that among 13 indexes for prediction, the minimum and maximum chest circumference, waistline and hipline fluctuate greatly, but MAE may not be the highest. The thigh circumference is 1.9cm and hipline is

1.8cm. This indicates to some extent that prediction precision of indexes is not fully controlled by fluctuation amplitude of the data length.

Experimental results about errors of different indexes of adult females are shown in Table 4. or MAE, the minimum is observed at wrist circumference and elbow circumference (0.5cm), and the maximum is achieved by the chest circumference (2.8cm). Elbow circumference presents the minimum mean error rate (2.3%), while the knee circumference shows the maximum mean error rate (5.0%). Knee circumference shows the maximum mean error rate and the maximum error. According to the observation of maximum error samples of the adult female dataset, it finds that samples

TABLE 4. Indexes and Errors of Adult Females.

| Error indexes	Neck circumference	Shoulder width	Chest circumference	Waistline	Hipline	Arm circumference
RMSE	1.6	1.9	3.5	2.7	3	1.2
MAE	1.2	1.6	2.8	2.1	2.3	1
Max error	5.9	4.8	10	8.8	12.8	3.4
Min error	0	0	0.02	0	0	0
Mean error rate	3.30%	4.40%	3.20%	2.90%	2.40%	3.90%
Elbow circumference	**Forearm circumference**	**Wrist circumference**	**Thigh circumference**	**Knee width**	**Calf circumference**	**Ankle circumference**
0.8	0.9	0.7	2.5	3.3	1.6	1
0.5	0.7	0.5	1.8	1.8	1.2	0.7
2.2	2.3	2.8	10.5	18.9	4.9	2.7
0	0	0	0	0.01	0	0
2.30%	3.20%	3.40%	3.40%	5.00%	3.50%	3.40%
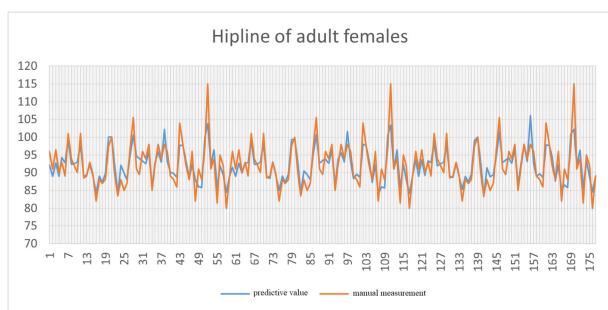
FIGURE 11. Comparison between predicted results and manual measurements of waistline of adult females.

with the maximum error differ significantly from samples with the secondary high error. Hence, the possibility of relative data anomaly caused by manual measurement error is not eliminated.

It can be seen from Table 3 and Table 4 that the total MAE of chest circumference, waistline and hipline is higher than those of the rest indexes, but the mean error rate may not be high. In addition, the comparison of the MAE of waistline of males and females reveals that the MAE of waistline of males is the highest, while the MAE of waistline of females is the smallest. This could be interpreted that the waist of males is more difficult to be identified than females and it is easy to cause mistakes during manual measurement.

It can be seen from broken line graphs of chest circumference, waistline and hipline in Figs.6-10 that manual measurement and predicted results generally keep a consistency. Generally, the consistence between broken line trends of manual measurement and predicted results is negatively correlated with MAE, which is proved by hipline of adult males in Fig.8.

V. CONCLUSION

In this article, we propose a noncontact, image-based method for measuring the human body parts for forensic applications in smart cities. We design our method to be noncontact and purely image-based so that the forensic evidence can be collected in an efficient manner. To address difficulties in size

measurement, low universality and poor convenience of existing noncontact anthropometry methods, a new end-to-end anthropometry method based on two views is proposed. The proposed method decreases error accumulation during the intermediate processes and it is easy for promotion. In the experiments, 15 indexes of body size are collected. Among them, the height and body weight are used as inputs and the rest 13 indexes are used as predictions. The error between the predicted results and manual measurement is calculated by an end-to-end method. According to our experimental results, there are some errors, but they can basically be kept within the mean error rate of 5%. This demonstrates that the proposed method can be used in practical noncontact anthropometry scenarios.

REFERENCES

[1] X. He, K. Wang, H. Huang, and B. Liu, "QoE-driven big data architecture for smart city," *IEEE Commun. Mag.*, vol. 56, no. 2, pp. 88–93, Feb. 2018.

[2] K. Wang, Y. Wang, Y. Sun, S. Guo, and J. Wu, "Green industrial Internet of Things architecture: An energy-efficient perspective," *IEEE Commun. Mag.*, vol. 54, no. 12, pp. 48–54, Dec. 2016.

[3] L. Qin and S. Xiaomei, "Research progresses on clothing anthropometry technology," *Modern Silk Sci. Technol.*, vol. 34, no. 6, pp. 32–34, 2019.

[4] C. Xu, K. Wang, Y. Sun, S. Guo, and A. Y. Zomaya, "Redundancy avoidance for big data in data centers: A conventional neural network approach," *IEEE Trans. Netw. Sci. Eng.*, vol. 7, no. 1, pp. 104–114, Jan. 2020.

[5] X. He, K. Wang, H. Huang, T. Miyazaki, Y. Wang, and S. Guo, "Green resource allocation based on deep reinforcement learning in content-centric IoT," *IEEE Trans. Emerg. Topics Comput.*, vol. 8, no. 3, pp. 781–796, Jul. 2020.

[6] X. He, K. Wang, and W. Xu, "QoE-driven content-centric caching with deep reinforcement learning in edge-enabled IoT," *IEEE Comput. Intell. Mag.*, vol. 14, no. 4, pp. 12–20, Nov. 2019.

[7] Z. Sayu, W. Anzi, and W. Shangmei, "Current conditions and development tendency of virtual fit platform," *Tianjin Textile Sci. Technol.*, vol. 5, no. 5, pp. 26–29, 2019.

[8] S. Petrak, D. Rogale, and V. Mandekic-Botteri, "Systematic representation and application of a 3D computer-aided garment construction method: Part II: Spatial transformation of 3D garment cut segments," *Int. J. Clothing Sci. Technol.*, vol. 18, no. 3, pp. 188–199, May 2006.

[9] P. Guan, L. Reiss, D. A. Hirshberg, A. Weiss, and M. J. Black, "DRAPE: DRessing any PErson," *ACM Trans. Graph.*, vol. 31, no. 4, pp. 1–10, Aug. 2012.

[10] X. Aijing and Z. Jie, "Research on key technology of virtual fit system," *Adv. Textile Technol.*, vol. 2020, no. 3, pp. 28–32, 2020.

[11] L. Ting, P. Xiaoyu, and T. Xiaohui, "Automatic measurement method of body size under a monocular depth camera," *Small Microcomput. Syst.*, vol. 40, no. 10, pp. 2202–2208, 2019.

[12] G. U. Bingfei, L. I. Xinhua, Z. Zhong, S. U. Junqiang, and G. Liu, "Girth fitting of young women based on body digital images," *J. Silk*, vol. 56, no. 08, pp. 46–51, 2019.

[13] R. A. Guler, N. Neverova, and I. Kokkinos, "DensePose: Dense human pose estimation in the wild," in *Proc. IEEE/CVF Conf. Comput. Vis. Pattern Recognit.*, Jun. 2018, pp. 7297–7306.

[14] H. Lu, X. He, M. Du, X. Ruan, Y. Sun, and K. Wang, "Edge QoE: Computation offloading with deep reinforcement learning for Internet of Things," *IEEE Internet Things J.*, vol. 7, no. 10, pp. 9255–9265, Oct. 2020.

[15] C. Xu, K. Wang, P. Li, R. Xia, S. Guo, and M. Guo, "Renewable energy-aware big data analytics in geo-distributed data centers with reinforcement learning," *IEEE Trans. Netw. Sci. Eng.*, vol. 7, no. 1, pp. 205–215, Jan. 2020.

[16] M. Dooley, "Anthropometric modeling programs-a survey," *IEEE Comput. Graph. Appl.*, vol. 2, no. 9, pp. 17–25, 1982.

[17] J. Bandouch, F. Engstler, and M. Beetz, "Accurate human motion capture using an ergonomics-based anthropometric human model," in *Proc. Int. Conf. Articulated Motion Deformable Objects*. New York, NY, USA: Springer, 2008, pp. 248–258.

[18] P. R. M. Jones and M. Rioux, "Three-dimensional surface anthropometry: Applications to the human body," *Opt. Lasers Eng.*, vol. 28, no. 2, pp. 89–117, Sep. 1997.

[19] T. B. Moeslund, A. Hilton, and V. Krüger, "A survey of advances in vision-based human motion capture and analysis," *Comput. Vis. Image Understand.*, vol. 104, nos. 2–3, pp. 90–126, Nov. 2006.

[20] K. M. Robinette, H. Daanen, and E. Paquet, "The CAESAR project: A 3-D surface anthropometry survey," in *Proc. 2nd Int. Conf. 3-D Digit. Imag. Modeling*, Oct. 1999, pp. 380–386.

[21] Z. Ben Azouz, M. Rioux, C. Shu, and R. Lepage, "Characterizing human shape variation using 3D anthropometric data," *Vis. Comput.*, vol. 22, no. 5, pp. 302–314, May 2006.

[22] Z. Ben Azouz, C. Shu, and A. Mantel, "Automatic locating of anthropometric landmarks on 3D human models," in *Proc. 3rd Int. Symp. 3D Data Process., Visualizat., Transmiss. (3DPVT)*, Jun. 2006, pp. 750–757.

[23] B. C. Munsell, A. Temlyakov, C. Qu, and S. Wang, "Person identification using full-body motion and anthropometric biometrics from kinect videos," in *Proc. Eur. Conf. Comput. Vis.* Florence, Italy: Springer, 2012, pp. 91–100.

[24] R. Tara, P. Santosa, and T. Adji, "Hand segmentation from depth image using anthropometric approach in natural interface development," *Int. J. Sci. Eng. Res*, vol. 3, no. 5, pp. 1–4, 2012.

[25] I. Stančić, J. Musić, and V. Zanchi, "Improved structured light 3D scanner with application to anthropometric parameter estimation," *Measurement*, vol. 46, no. 1, pp. 716–726, Jan. 2013.

[26] M. Robinson and M. Parkinson, "Estimating anthropometry with microsoft Kinect," in *Proc. 2nd Int. Digit. Hum. Modeling Symp.*, vol. 1, no. 2, 2013, pp. 1–7.

[27] P. Meunier and S. Yin, "Performance of a 2D image-based anthropometric measurement and clothing sizing system," *Appl. Ergonom.*, vol. 31, no. 5, pp. 445–451, Oct. 2000.

[28] I. Stancic, T. Supuk, and M. Cecic, "Computer vision system for human anthropometric parameters estimation," *WSEAS Trans. Syst.*, vol. 8, no. 3, pp. 430–439, 2009.

[29] S. Gupta, M. K. Markey, and A. C. Bovik, "Anthropometric 3d face recognition," *Int. J. Comput. Vis.*, vol. 90, no. 3, pp. 331–349, 2010.

[30] L. Shunhua and W. Jianping, "Exploration on noncontact anthropometry method based on two-dimensional images," *J. Textile Res.*, vol. 34, no. 8, pp. 151–155, 2013.

[31] C. Barron and I. A. Kakadiaris, "Estimating anthropometry and pose from a single image," in *Proc. IEEE Conf. Comput. Vis. Pattern Recognit. CVPR*, Jun. 2000, pp. 669–676.

[32] C. Barrón and I. A. Kakadiaris, "Estimating anthropometry and pose from a single uncalibrated image," *Comput. Vis. Image Understand.*, vol. 81, no. 3, pp. 269–284, Mar. 2001.

[33] C. Barron and I. A. Kakadiaris, "On the improvement of anthropometry and pose estimation from a single uncalibrated image," *Mach. Vis. Appl.*, vol. 14, no. 4, pp. 229–236, Sep. 2003.

[34] T. Fei, "Research body shapes of young women based on digital images and noncontact two-dimensional measurement system," M.S. thesis, Dept. Fashion Des. Eng., Suzhou Univ., Suzhou, China, 2010.

[35] J. Kaichen, "Circumference fitting based on two-dimensional noncontact measurement system of young men," M.S. thesis, Dept. Textile Eng., Suzhou Univ., Suzhou, China, 2014.

[36] Y. Zongqin and W. Qinhua, "Research on image size measurement technology of two-dimensional human photography," *Ind. Technol. Vocational Educ.*, vol. 16, no. 2, pp. 14–15, 2018.

[37] Z. Kun, M. Li, and L. Rong, "Noncontact anthropometry method based on images," *Comput. Eng. Design*, vol. 38, no. 002, pp. 511–516, 2017.

[38] X. Jiayan and K. Caiyuan, "Effects of body feature parameters on remote anthropometric precision," *Silks*, vol. 56, no. 8, 2019.

[39] H. Xiuli, "Research on measurement system for young women based on digital images," M.S. thesis, Dept. Fashion Des. Eng., Suzhou Univ., Suzhou, China, 2009.

[40] J. Friedman, "Greedy function approximation : A gradient boosting machine," *Ann. Statist.*, vol. 29, no. 5, pp. 1189–1232, 2001.

[41] E. Shelhamer, J. Long, and T. Darrell, "Fully convolutional networks for semantic segmentation," *IEEE Trans. Pattern Anal. Mach. Intell.*, vol. 39, no. 4, pp. 640–651, Apr. 2017.

[42] T. Chen and C. Guestrin, "XGBoost: A scalable tree boosting system," in *Proc. 22nd ACM SIGKDD Int. Conf. Knowl. Discovery Data Mining*, Aug. 2016, pp. 785–794.

GE XU received the Ph.D. degree in artificial intelligence from Peking University, Beijing, China. He is currently an Associate Professor and an Associate Dean (Research) of the College of Computer and Control Engineering, Minjiang University, Fuzhou, China. He is also with the College of Mathematics and Computer Science, Fuzhou University, Fuzhou. His research interests include computer vision, natural language processing, and pattern recognition.

YONGQIANG XIAO received the B.E. degree from the School of Computer Science and Engineering, Wuhan Institute of Technology, Wuhan, China, in 2017, and the M.E. degree from the College of Mathematics and Computer Science, Fuzhou University, and also from the College of Software. He was also a member of the Artificial Intelligence School Enterprise Joint Laboratory between the Industrial Design and Research Institute, Minjiang University, and Fuzhou Kaopuyun Technology Co., Ltd. He is currently an Engineering Researcher with Fuzhou Kaopuyun Technology. His research interests include artificial intelligence and multimodal understanding.
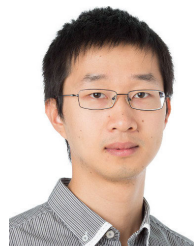
TAO WANG (Member, IEEE) received the B.E. degree in information engineering from the South China University of Technology, Guangzhou, China, in 2009, and the Ph.D. degree in computer science from The Australian National University, Canberra, ACT, Australia, in 2016. He was also a member of the Computer Vision Research Group, National ICT Australia, Canberra. He is currently a Lecturer with the College of Computer and Control Engineering, Minjiang University, Fuzhou, China. He is also with the College of Mathematics and Computer Science, Fuzhou University, Fuzhou, and also with The Key Laboratory of Cognitive Computing and Intelligent Information Processing of Fujian Education Institutions, Wuyi University, Wuyishan, China. His research interests include scene understanding, object detection, and semantic instance segmentation.

YIN GUAN received the Ph.D. degree in fundamentals of artificial intelligence from Xiamen University, Xiamen, China, in 2012. He is currently a Teacher and a Senior Engineer with the College of Computer and Control Engineering, Minjiang University, Fuzhou, China. His current research interests include application of machine learning and artificial intelligence in music and sound.

JINHUA XIAO is currently the Chief Technology Officer of Fuzhou Kaopuyun Technology Co., Ltd. He has more than 15 years of experiences in cloud computing, big data, artificial intelligence, and related industries.
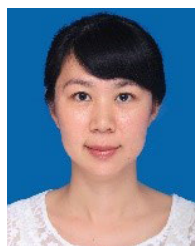
ZHIXIONG ZHONG (Member, IEEE) received the B.S. degree in mechatronics and the M.S. degree in control theory and control engineering from Fuzhou University, Fuzhou, China, in 2008 and 2012, respectively, and the Ph.D. degree from the Research Institute of Intelligent Control and Systems, Harbin Institute of Technology, Harbin, China, in 2015. In 2013, he was a Visiting Student with the Department of Mechanical Engineering, University of Victoria, Canada. In 2018, he joined the School of Computer and Control Engineering, Minjiang University, Fuzhou. He is currently a Professor with Minjiang University. He has published more than 25 articles in journals, conferences, and books and authored the book *Large-Scale Fuzzy Interconnected Control Systems Design and Analysis* (Pennsylvania: IGI Global) and the book *Modeling, Control, Estimation, and Optimization for Microgrids: A Fuzzy-Model-Based Method* (London: CRC Press). His articles have been cited more than 150 times (according to Reseachgate). His research interests include fuzzy control, robust filtering, and large-scale control.

DONGYI YE received the Ph.D. degree in applied mathematics from Paul Sabatier University, Toulouse, France, in 1992. He is currently a Professor with the College of Mathematics and Computer Science, Fuzhou University, Fuzhou, China. His research interests include machine learning, computer vision, and pattern recognition.

JIA LYU received the Ph.D. degree in fashion design and fashion engineering from Jiangnan University, China, in 2014. She is currently an Associate Professor with the College of Clothing and Artistic Engineering, Minjiang University, China. Her research interests include modern fashion technique and emotional fashion design based on human–computer interaction.

• • •